Current Applied Science and Technology e-ISSN: 2586-9396

Curr. Appl. Sci. Technol. 2026, Vol. 26 (No. 1), e0263975

Research article

Photorefractive Effect in an Imperfect Cerium Doped Barium Titanate Crystal: Reflection Grating Case

Wasuphon Khotphuthon[1], Suwan Plaipichit[2], Suebtarkul Suchat[3] and Prathan Buranasiri[1]*

[1]Department of Physics, School of Science, King Monkut's Institue of Technology Ladkrabang, Bangkok, Thailand
[2]Department of Physics, Faculty of Science, Srinakharinwirot University, Bangkok, Thailand
[3]Faculty of Science and Technology, Phranakhon Rajabhat University, Bangkok, Thailand

Received: 7 August 2024, Revised: 26 February 2025, Accepted: 6 March 2025, Published: 29 May 2025

Abstract

The photorefractive (PR) effect, a nonlinear optic phenomenon, occurs in materials that have electro-optic (EO) properties. When two coherent beams of light interfere with each other in a PR material, donor electrons between valence band and conduction band, caused by material impurity, absorb the photon and are excited into the conduction band and generate electron-hole pairs. This process induces a periodic electric field called a space charge field that alters the material's refractive index due to the EO effect. In this research, we explored reflection grating (RG) in an imperfect Ce-doped $BaTiO_3$ crystal and then showed optical image correlation using the RG. Two beam coupling was investigated using two non-Gaussian incident beams on the opposite surface of an imperfect Ce-doped $BaTiO_3$ crystal. Light at green wavelengths from a semiconductor laser was used as the source of the incident beams and entered at certain angles relative to the crystal c-axis. Large beam coupling power was observed in both incident directions when the angle between both incident beams is at Bragg's angle in the direction of the c-axis. The diffraction light was found to be in the same polarization as the incident beam. In addition, interesting results for the optical correlation using reflection grating were demonstrated. These results suggest that by doping $BaTiO_3$ with cerium, strong beam coupling or photorefractive grating can be observed with certain incident writing angles on the crystal, which could be utilized in future flexible holographic devices in the future.

Keywords: photorefractive effect; two-wave coupling; reflection grating; transmission grating; optical image correlation

1. Introduction

Barium titanate crystal is one of the most popular photorefractive (PR) materials (Yeh, 1933). Phase conjugation, isotropic and anisotropic beam coupling have been observed in $BaTiO_3$ crystals. Two wave coupling (TWC) has been used for exploring the figure of merit of PR materials. The energy transfer between two incident beams (the power of one

*Corresponding author: E-mail: prathan.bu@kmitl.ac.th
https://doi.org/10.55003/cast.2025.263975

incident light transferred to another incident light by diffraction on the grating) in PR TWC exists due to the combination of induced refractive index and the phase shift between the intensity profile and the induced refractive index profile. Recently, group delay in telecom wavelength was performed using TWC (Bouldja et al., 2023). PR $BaTiO_3$ crystals have often been used for dynamic grating applications. Due to their large electro-optic coefficient r_{42}, they generate large beam coupling which can be used for optical information processing applications. However, the crystal response time is slow and in addition, large beam fanning is easily generated, which reduces the benefit of the applications as image quality is the degraded. After doping with impurities such as cerium or rhodium at appropriate concentrations, the PR properties such as response time and resolution were improved (Yang et al., 1995; Petris et al., 2000). The application of the PR effect in Ce-doped $BaTiO_3$ crystals has been of interest for some time (Buranasiri et al., 2003; Plaipichit et al., 2012). Different phenomena due to the PR effect had been explored when the crystal was still in its perfect shape without any crack by using Gaussian beam from gas lasers (He-Ne laser and Ar+ ion laser). Recently, strong TWC due to the transmission grating in the same Ce-doped $BaTiO_3$ crystal was observe (Khotphuthon et al., 2024) after it was cracked due to falling. The imperfect crystal here is the cracked crystal. In this paper, TWC due to the reflection grating in an imperfect crystal is presented.

The photorefractive (PR) effect is a phenomenon in electro-optic (EO) materials where the index of refraction of a material is changed due to the interference of light on the material. The periodic pattern of the interference of light induces the index grating due to the PR effect. The gradient intensity of light on the EO crystal generates charge density, which creates a space charge field and then creates index variation. Grating formation due to the PR effect can be explained by the band transport model or Kukhtarev equations, which consist of four equations (Yeh, 1933).

Equation 1: The rate equation for donor impurity ionization

$$\frac{\partial {N^i}_D}{\partial t} = sI({N_D} - {N^i}_D) - \gamma_R N {N^i}_D \tag{1}$$

where $N, {N^i}_D, s, I$ and γ_R are electron density, electron density ionized, cross-section for photoexcitation, intensity of incident light, and recombination coefficient.

Equation 2: The rate equation for electron density creation

$$\frac{\partial N}{\partial t} - \frac{\partial {N^i}_D}{\partial t} = \frac{1}{q}\nabla \cdot j \tag{2}$$

where q, j are electron charge and current density, respectively.

Equation 3: The current density is composed of two phenomena, drift and diffusion

$$j = qN\mu E + k_B T_\mu \nabla N \tag{3}$$

where $\mu, E, k_B T$ are mobility tensor, electric field, Boltzmann constant and temperature, respectively.

Equation 4: The Poisson equation

$$\nabla \cdot \epsilon E = \rho(r) = -q(N + N_A - N^i{}_D) \tag{4}$$

where ϵ, ρ, N_A are dielectric sensor, charge density, and acceptor impurity, respectively.

For two-wave coupling of PR reflection grating, in this experiment, two wave coupling (TWC) due to reflection grating in an imperfect PR cerium doped barium titanate crystal was observed. In this research, two incident beams are diffracted by an induced reflection grating to the direction of the other beam, as shown in Figure 1. The angle of PR grating is parallel to the $\hat{c}$-axis and the angle between incident beams equal to $\hat{\theta}/2$. The reflection coupling constant due to the PR reflection grating can be written in equation 5 (Honda et al., 1993) as follows.

$$\Gamma = \frac{2\pi r_{eff}}{n} \frac{E_q E_d}{E_q + E_d} \tag{5}$$

where n, r_{eff}, E_q, E_d are index of refraction, effective electro-optic coefficient, space charge field, and diffusion gradient field, respectively. The r_{eff} can be written as shown in equation 6.

$$r_{eff} = r_{13} cos\, \beta cos^2 \alpha - r_{42} sin\, \beta\, sin\, \alpha\, cos\, \alpha + r_{33} \cos \beta\, sin^2 \alpha \tag{6}$$

where β is the angle between the space charge field and the c-axis, α is the angle of the direction of the incident beam and the c-axis. The space charge field and the diffusion gradient field are the sources which generate PR grating.

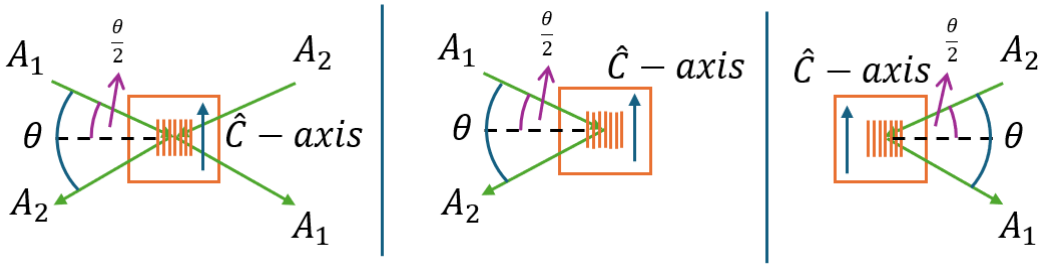

Figure 1. Two-wave coupling due to the diffracted light from reflection grating

Optical image correlation OMC has been of interest in the research community due to its usefulness when identifying and recognizing images and signals (Jain, 1989). The application of PR materials has been of interest as it involves implementation of OMC in real time. The search for new PR applications for OMC has been actively continued by different material research groups. PR volume transmission grating and reflection grating have been explored for novel PR material searching. Recently, the analysis of a PR correlator was studied using complicated images with different figures of merit (Nehmetallah et al., 2016). The traditional joint transform correlation (JTC) between two images $s(x, y)$ and $t(x, y)$ is written in equation 7 (Goodman, 2017) as follows.

$$A_{JTC} = FT^{-1}\left\{\left|S(f_x, f_y) + T(f_x, f_y)\right|^2\right\} \quad (7)$$

where $S(f_x, f_y) = FT\{s(x,y)\}$, $T(f_x, f_y) = FT\{t(x,y)\}$, $FT(\cdot)$ denotes the Fourier transform of the signals, (x, y) are spatial coordinates and (f_x, f_y) are frequency coordinates. In the following sections, first the experimental methods for observing reflection grating in Ce-doped $BaTiO_3$ crystal was explained. Then, the experimental results were shown and discussed. Finally, the OMC results using self-diffraction reflection grating are also shown. The OMC image is the JTC between the PR grating and the image of the unblocked beam.

2. Materials and Methods

2.1 $BaTiO_3$ and cerium-doped $BaTiO_3$

$BaTiO_3$ is one of important PR crystal (Feinberg et al., 1980; Yang et al., 1995): however, these crystals have slow response time and strong beam fanning effect. Usually, the undoped PR $BaTiNO_3$ is doped with Fe^{2+} or Fe^{3+} and the bandgap is changed in proportion to the Fe concentration. The PR effect needs donor or acceptor energy levels otherwise there is no generation of space charge field due to drift and diffusion of electrons or holes in the visible light regime. In undoped crystal, the electro-optic gain coefficient, the absorption coefficient, and total effective trap density are small in the visible light regime so an experiment for observing the PR effect in the crystal requires a lot of precision with optical alignment and exact light power. Due to its fast response time, a Ce-doped $BaTiO_3$ single crystal is a good choice for PR effect applications. The Ce-doped $BaTiO_3$ single crystals are prepared by famous top seeded solution growth (TSSG) technique and the CeO2 dopant to the melt of BaTiO3 was added. The level of Ce-doped energy is in between the valence band and conduction band. In Ce-doped crystal, the electro-optic gain coefficient, the absorption coefficient, and total effective trap density at wavelength larger than 514 increase with the concentration of cerium. With increasing of those properties, the Ce-doped crystal has fast response time on photorefractive behavior when we use the light in this regime (Yang et al., 1995).

2.2 The experimental methods

We used unpolarized wavelength 532 nm from a semiconductor laser for our light source. The beam was separated into two paths with a beamsplitter. One path of the non-polarized laser light was propagated onto a mirror and reflected through a lens to focus the beam onto a $\mathrm{Ce-doped\ BaTiO_3}$ of dimensions $a \times b \times c = 5.6\ \mathrm{mm} \times 5.6\ \mathrm{mm} \times 6.4\ \mathrm{mm}$ on the Y side of the crystal, as shown in Figure 2. The other path of light was propagated onto a second mirror and reflected through a lens to the X side of the crystal, which was opposite to the Y side. The angle between the two beams was varied, with certain angles giving larger degrees of beam diffraction. The interference of the incident beams generated reflection grating which was parallel to the C-axis. A power meter was put for measuring the power of the diffracted light, as shown in Figure 2. It should be note that the C-axis is the axis that is parallel to the crystal symmetry.

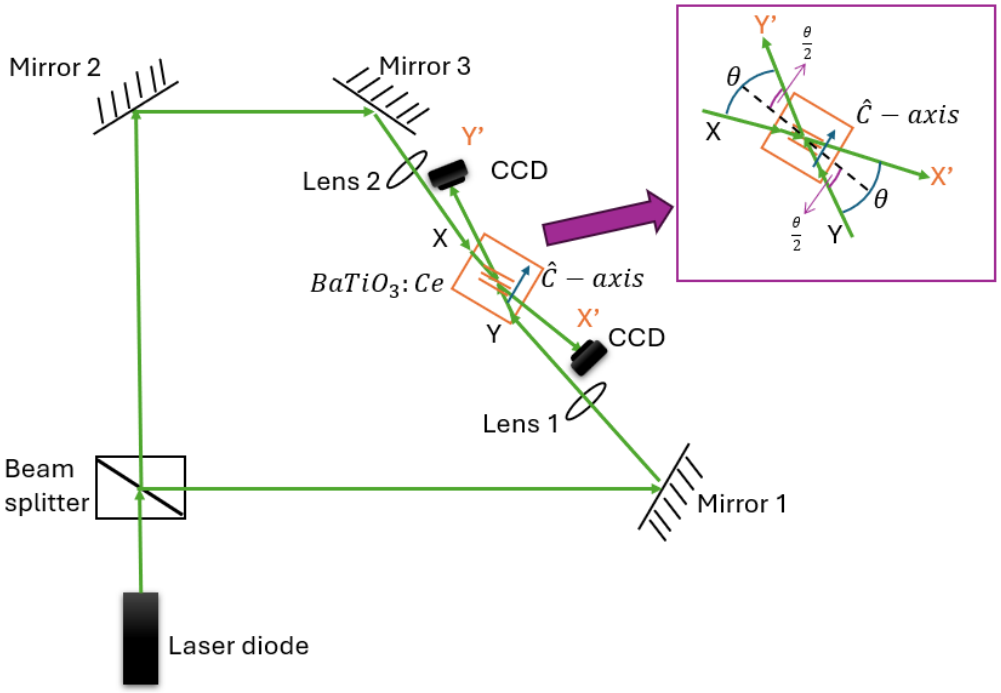

Figure 2. Experimental setup for observing TWC intensity

In the first experimental setup, the optimum angles for incident beams were explored. We varied a number of angles between the incident beams, creating some strong reflection grating with large intensity of diffracted beams, and the direction of C-axis affected the diffracted light of incident beams. To measure energy of diffracted intensity, we blocked one of incident beams in the direction of X or Y for observing the beam transfer from TWC phenomena by reflection grating, as shown in Figure 3.

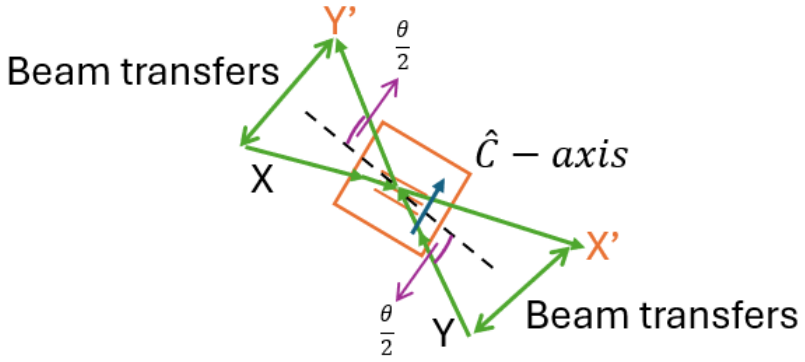

Figure 3. Beam transferring from TWC using reflection grating (Y′ and X′ are the direction of diffracted beams.) The double headed arrows show a beam can transfer from X to Y or Y to X directions.

In the second experimental setup, we put a sample object slide between mirror 2 and mirror 3, and then we used a CCD camera instead of photodetector to record correlated images (Figure 4). This is called optical image correlation (OIC) using self-diffraction.

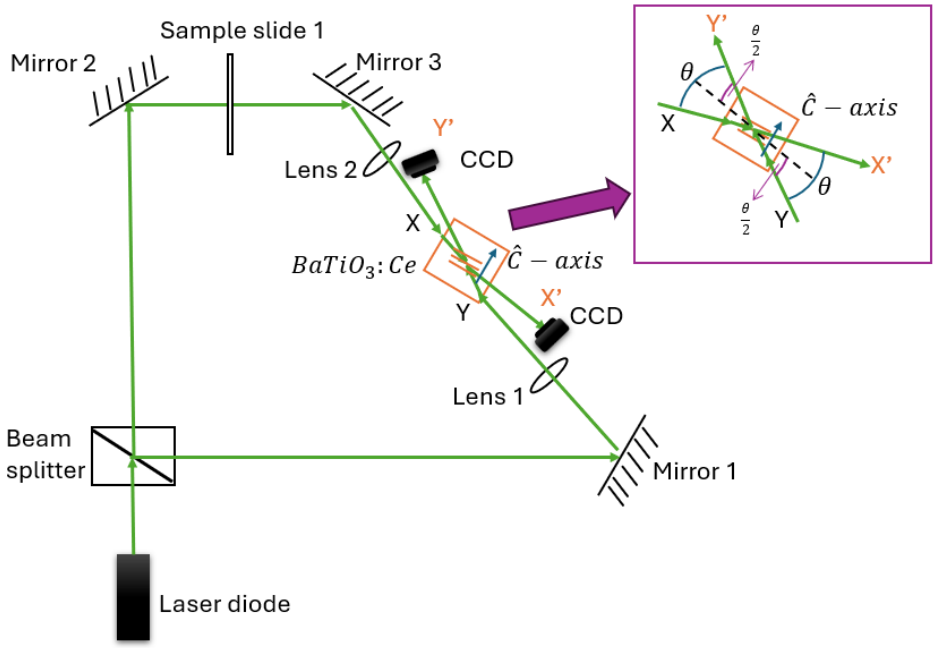

Figure 4. Optical image correlation experimental setup. The setup was the same as in Figure 2 but the sample slides were insert between mirror 2 and mirror 3. A CCD camera was used to capture the image correlation.

3. Results and Discussion

3.1 Diffraction from reflection grating

The results for diffraction power of different angles of incident beams are shown in Table 1. First, we measured the power of the transmission beams without blocking any incident beams. Next, we measured the power of the diffracted beams by blocking one incident beam and measuring the power of the diffracted beam of another incident beam, i.e. we blocked beam in X/Y direction and measured the power of beam in X′/Y′ direction as shown in Figure 4. We did the same with the other incident beam. To do this, we observed the diffracted light of the unblocked beam by the generated reflection grating. A polarizer was inserted at the input beam and output beam to find the polarization of the incident and diffracted beams. From the experimental results, diffracted light was observed when the angles between the incident beams were certain large angles (55°, 60°, and 65°) (Figures 5-7) and the polarization of diffracted light was in the same direction of incident light, while

Table 1. powers of diffracted beams with and without blocking incident beams

Angle between Incident Beams	Direction of the Incident Beams as shown in Figure 1	Power of Transmission Beams (nW) (Without blocking of incident beams)	Power of Diffracted Beams (nW) (With blocking of incident beams)
A (55°)	X′	107.8	0.68
	Y′	51.4	1.08
B (60°)	X′	155.4	0.09
	Y′	74.2	3.21
C (65°)	X′	199.7	1.08
	Y′	157.8	2.26

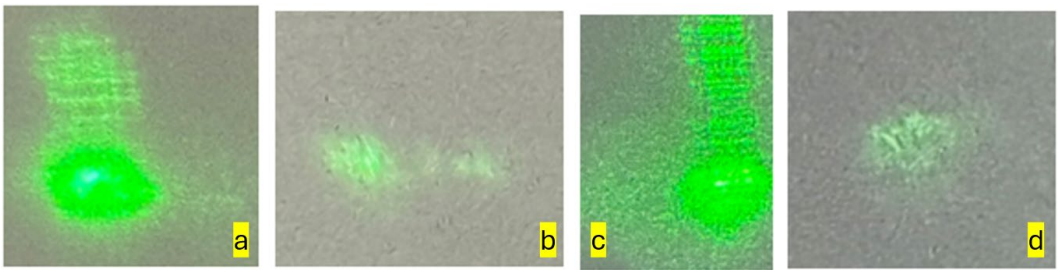

Figure 5. Images of diffracted beams for incident angle of 55°
(a) without blocking the incident light in Y′ direction, (b) with blocking the incident light in Y′ direction, (c) without blocking the incident light in X′ direction, and (d) with blocking the incident light in X′ direction

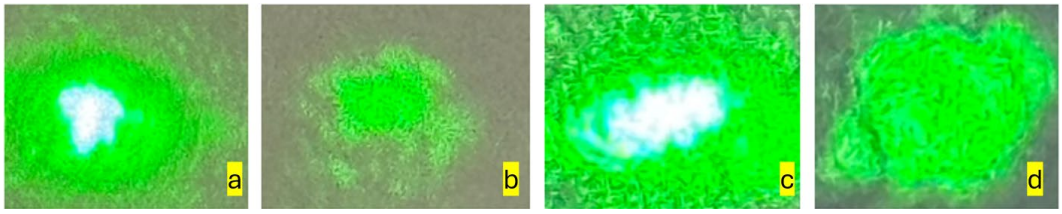

Figure 6. Images of diffracted beams for incident angle of 60°
(a) without blocking the incident light in Y′ direction, (b) with blocking the incident light in Y′ direction, (c) without blocking the incident light in X′ direction, and (d) with blocking the incident light in X′ direction

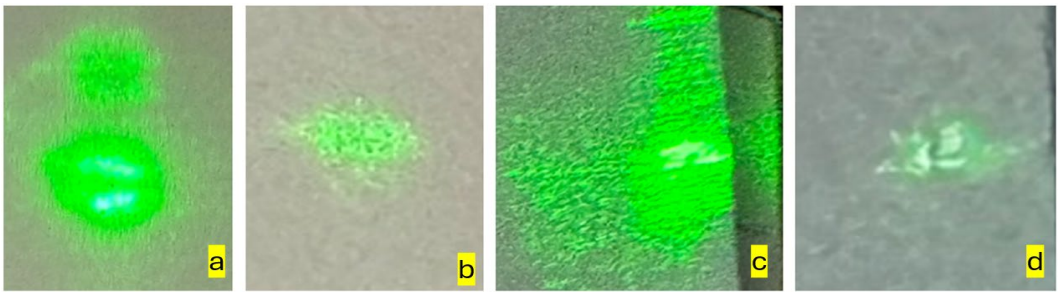

Figure 7. Images of diffracted beams for incident angle of 65°
(a) without blocking the incident light in Y′ direction, (b) with blocking the incident light in Y′ direction, (c) without blocking the incident light in X′ direction, and (d) with blocking the incident light in X′ direction

for transmission grating, the angle between the incident light were at some small angles and the polarization of diffracted beam was perpendicular to the incident beam (Kukhtarev et al., 1984). Although TWC was observed in both transmitted directions of the incident beams, the TWC was large in the direction of the incident beam that made a small angle with the C-axis direction, as supported by equation 6. The power of beam in direction X′ was found to be less than the power of the beam in direction Y′ when we blocked the X and Y beams, respectively. From our point of view, the crack on the crystal only affected the macroscopic properties of the crystal (geometrical optics), and it did not affect the microscopic properties of the crystal (quantum regime). From our investigation, phase conjugate beams were not generated since the cracks in the crystal deflected the light to other unwanted directions. The generation of a phase conjugate (PC) beam requires the assistance of a resonator, which can be the crystal structure or an outside resonator and the damage inside the crystal made it difficult to be a suitable resonator.

3.2 Optical image correlation using self-reflection grating

In this section, we show the optical image correlator (OMC) performance using self-reflection grating. Two different samples, monocotyledon stem and onion epidermis were used as objects for OMC. In this experiment, the angle between the two incident beams selected was 60° since it gave the strongest TWC in the first experiment. First, the monocotyledon stem was put in the path of an incident beam (as shown in Figure 4), and then we observed the OMC of diffraction in the X′ direction and Y′ direction, as shown in Figure 8. Next, we did the same with the onion epidermis. The OMC of the onion epidermis is shown in Figure 9. In the end, we put both samples in both paths of the incident beams and investigated the OMC performance in the X′ direction and Y′ direction, as shown in Figure 10. From the experimental results, we observed the OMC clearly in both X′ and Y′ diffracted directions. The future goal of this work is to investigate OMC with more different samples and apply machine learning to manage sparse images of OMC. The combine theory of OMC using transmission grating and reflection grating need to be done.

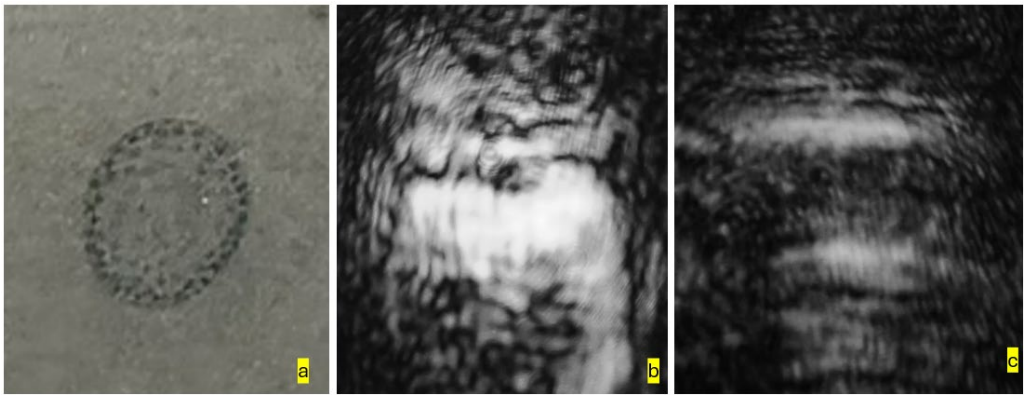

Figure 8. Optical image correlation using reflection grating of monocotyledon stem (a) sample, (b) image of diffraction in X′-direction, and (c) image of diffraction in Y′-direction

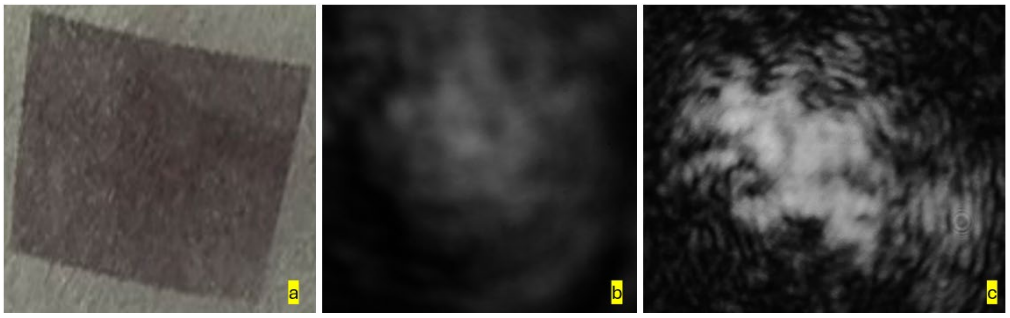

Figure 9. Optical image correlation using reflection grating of onion epidermis (a) sample, (b) image of diffraction in X′-direction, and (c) image of diffraction in Y′-direction

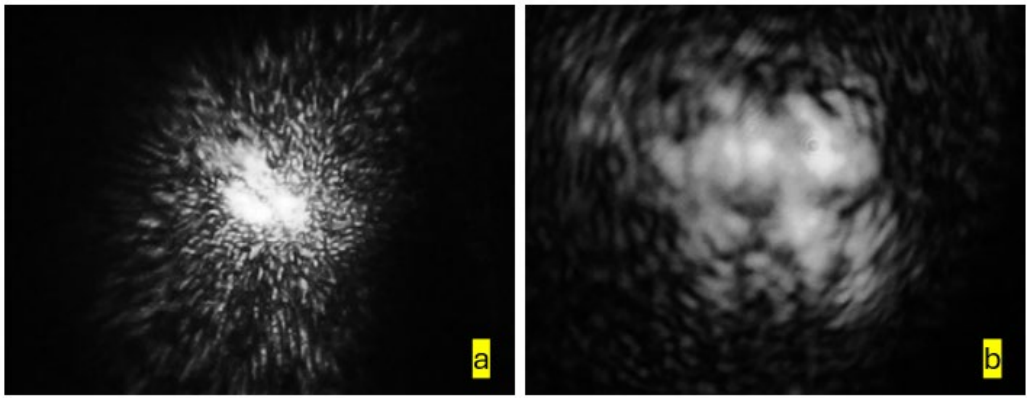

Figure 10. Optical image correlation using both sample in each incident beam (a) onion epidermis in X′-direction, (b) monocotyledon stem in Y′-direction

4. Conclusions

In this research, the reflection grating was generated from two incident light beams on opposite direction of a cracked cerium doped barium titanate crystal. Although the crystal was imperfect, the TWC results observed were the same as those seen when the crystal was intact. Large powers of diffraction beams were found at certain large angles, i.e. 55°, 60°, and 65° degrees between the two incident beams on opposite surfaces of the crystal. Although the diffraction beams were observed on both directions of incident beams, the diffracted beam in the direction of the incident beam which made small angle with direction of $\hat{c}$ axis was larger. The polarization of the diffracted beam was the same as the incident beam. The image correlation using the diffracted beam was explored as well. Clear correlation images were also recorded and these are subject of interest for future research. From our results in this research and the results from transmission grating, the photorefractive effect of barium titanate was improved by doping with cerium and the crystal may be suitable for the application in dynamic holography in the future.

5. Authors' Contributions

Wasuphon Khotphuthon: designed and performed experimental setup, collected and analyzed experimental results, drafted and wrote the manuscript. Suwan Plaipichit: suggested the concept idea and experimental method, read and edited the manuscript. Suebtarkul Suchat: extensive suggested the experimental approach, reviewed and edited the manuscript. Prathan Buranasiri: supervised and conceived this project. designed and performed experimental setup. collected and analyzed experimental results. drafted, reviewed, and edited the manuscript.

6. Conflicts of Interest

The authors declare that they have no conflicts of interest.

ORCID

Prathan Buranasiri https://orcid.org/0000-0001-7071-3194

References

Bouldja, N., Sciamanna, M., Grabar, A., & Wolfersberger, D. (2023). Zero-broadening slow light from photorefractive two-wave mixing. *Optics Letters*, 48(18), 4853-4856. https://doi.org/10.1364/OL.496327

Buranasiri, P., Banerjee, P. P., Polejaev, V., & Sun, C.-C. (2003). Image correlation using isotropic and anisotropic higher-order generation, and mutually pumped phase conjugation in photorefractive barium titanate. *Proceedings of SPIE*, 5206, 215-222. https://doi.org/10.1117/12.508595

Feinberg, J., Heiman, D., Tanguay, A. R. Jr., & Hellwarth, R. W. (1980). Photorefractive effects and lightinduced charge migration in barium titanate. *Journal of Applied Physics*, 51, 1297-1305. https://doi.org/10.1063/1.327824

Goodman, J. W. (2017). *Introduction to Fourier optic*. 4th ed. Roberts and Company.

Honda, T., Yamashita, T., & Matsumoto, H. (1993). Self-pumped phase conjugation with $BaTiO_3$ in a reflection-grating ring configuration. *Optics Communications*, 103(5-6), 434-438. https://doi.org/10.1016/0030-4018(93)90170-A

Jain, A. (1989). *Fundamentals of digital ımage processing*. Prentice-Hall.

Khotphunthon, W., Plaipichit, S., & Buransiri, P. (2024). Two-beam coupling in imperfect photorefractive cerium doped barium titanate crystal. *Asian Journal of Physics*, 33(7&8), 429-434. http://doi.org/10.54955/AJP.33.7-8.2024.429-434

Kukhtarev, N. Kratzig, E. Kulich, H. (1984). Anisotropic self-diffraction in $BaTiO_3$. *Applied Physics*, 35(1), 7-11.

Nehmetallah, G., Khoury, J., Alam, M., & Banerjee, P. P. (2016). Photorefractive two beam coupling joint transform correlator: modelling and performance evaluation. *Applied Optics*, 55(15), 4011-4023. https://doi.org/10.1364/AO.55.004011

Petris, A., Damzen, M. J., & Vlad, V. I. (2000). Enhanced wave mixing in photorefractive rhodium-doped barium titanate crystals. *Optics Communications*, 176(1-3), 223-229. https://doi.org/10.1016/S0030-4018(00)00475-2

Plaipichit, S., Buranasiri, P., Nuansri, R., & Neeyakorn, V. (2012). Multi high-order anisotropic self-diffraction in cerium doped $BaTiO_3$ crystal. In *Proceedings of SPIE, 8258, organic photonic materials and devices XIV* (pp. 82581H). Society of Photo-Optical Instrumentation Engineers. https://doi.org/10.1117/12.908574

Yang, C., Zhang, C., Yeh, P., Zhu, Y., & Wu, X. (1995). Photorefractive properties of Ce: $BaTiO_3$ crystals. *Optics Communications*, 113(4-6), 416-420. https://doi.org/10.1016/0030-4018(94)00524-X

Yeh, P. (1993). *Introduction to photorefractive nonlinear optics*. Wiley Intersciene.